PCCP

Cite this: *Phys. Chem. Chem. Phys.*, 2011, **13**, 5413–5421

www.rsc.org/pccp

PAPER

Effects of applied potential on the mass of non-conducting poly(*ortho*-phenylenediamine) electro-deposited on EQCM electrodes: comparison with biosensor selectivity parameters

Sharon A. Rothwell and Robert D. O'Neill*

Received 1st November 2010, Accepted 22nd February 2011
DOI: 10.1039/c0cp02341h

An electrochemical quartz-crystal microbalance (EQCM) was used to determine the mass of poly-(*o*-phenylenediamine) (PoPD) layers electro-deposited at different applied potentials in neutral buffered monomer solution, conditions that produce the insulating form of the polymer used as a permselective membrane in biosensor applications. There was a systematic increase in the total, steady state PoPD mass deposited for fixed applied potentials from 0.05 to 0.6 V *vs.* SCE, followed by a plateau up to 0.8 V. Comparison of PoPD mass and permselectivity parameters indicates that the ability of the passivating form of PoPD to block interference species in biosensor applications is not related in a simple way to the mass of material deposited on the surface. Instead, effects of the applied electropolymerisation potential in driving the electro-oxidation of oPD dimers and oligomers formed during the electro-deposition process are likely to have a more direct impact on the selectivity characteristics of the PoPD layer. The results highlight the usefulness of apparent permeabilities, especially of ascorbic acid, in revealing differences between PoPD layers electro-deposited under different conditions.

1. Introduction

From the first description of an enzyme-modified electrode to monitor concentration dynamics of a specific analyte,[1] through initial attempts at theoretical descriptions of the behaviour of these 'biosensors',[2,3] their application as analytical tools is continuing to grow and diversify in areas such as environmental surveillance, batch food analysis and clinical monitoring, and is beginning to impact on quality-of-life issues.[4–8] Depending on the target analyte, different signal transduction pathways have been exploited in the design of enzyme-based biosensors, including direct oxidation of reduced oxidases,[9–11] dehydrogenase chemistries,[12–14] redox mediators,[15–17] and spectrophotometric approaches.[18–20] However, 'first generation' electrochemical biosensors remain the most common strategy for many applications,[21–25] the majority being oxidase-based devices designed to operate in amperometric mode, detecting H_2O_2 generated by the reaction of co-substrate (dioxygen) with the reduced form of the enzyme (reactions (1)–(3)).

$$\text{Substrate} + \text{Ox/FAD} \rightarrow \text{Products} + \text{Ox/FADH}_2 \quad (1)$$

$$\text{Ox/FADH}_2 + \text{O}_2 \rightarrow \text{Ox/FAD} + \text{H}_2\text{O}_2 \quad (2)$$

$$\text{H}_2\text{O}_2 \rightarrow \text{O}_2 + 2\text{H}^+ + 2\text{e}^- \quad (3)$$

UCD School of Chemistry and Chemical Biology, University College Dublin, Belfield, Dublin 4, Ireland. E-mail: Robert.ONeill@UCD.ie

First-generation biosensors in general, and especially those designed for tissue implantation,[26–30] must be capable of effective rejection of electroactive interference by endogenous reducing agents in the target medium, because these devices are normally operated at a high applied overpotential for efficient H_2O_2 detection (reaction (3)). Thus, the analyte specificity of enzyme-based amperometric biosensors can be seriously undermined by high levels of interference species such as ascorbic acid (AA), a ubiquitous anti-oxidant present at relatively high concentrations (0.1–10 mM) in biological fluids.[31] Even when significantly lower applied overpotentials can be used for direct H_2O_2 oxidation,[32,33] AA interference can persist because of its very low redox potential.[34,35] The alternative strategy of H_2O_2 electroreduction[36–38] is also prone to interference, in this case by reduction of molecular oxygen present in the target medium,[39] although electrocatalytic reduction of H_2O_2 at $\sim$0 V *vs.* SCE appears to offer a window of minimum interference.[17,40–42]

There is a real need, therefore, for continued improvements in biosensor selectivity for biological applications. Permselective membranes,[21,43] or other strategies such as fine-tuning the operational applied potential,[17,41,44] are often an essential strategy for reliable biosensor monitoring of biological, and other complex, matrices. Electrosynthesised poly-phenylene-diamines (PPDs) have been widely reported to possess excellent permselective properties relevant to biosensor applications, being highly permeable to H_2O_2 and efficient blockers

of interference compounds.[45–54] The best of the three isomeric forms of the monomer for polymer formation in biosensor fabrication is still open to debate,[46,47,55] and this may depend on the nature of the intended application.[56,57] PPD formed from the *ortho* isomer (PoPD) remains the most studied form for biosensor applications,[41,52,53,58–66] and is the subject of the present study.

The physicochemical phenomena associated with the electrosynthesis of surface-deposited polymers in general, and PPDs in particular, are extensive and complex.[67] Factors involved include: the nature of the first electron transfer step;[68] following chemical reactions with unreacted and oxidised monomer;[68,69] subsequent oxidation of soluble products, surface deposition of insoluble oligomers, and possible further oxidation of deposited molecules;[69–71] pH and background electrolyte effects;[69,72–74] and the influence of the applied potential used in the electro-deposition process.[69,74,75] Recently, we demonstrated that the applied electropolymerisation potential strongly affected the permselective properties of PoPD,[75] which fell into three distinct ranges: very poor for mild anodic values (<0.2 V *vs.* SCE), indicating little or no PoPD coating formed on the electrode surface; moderate when the PoPD was generated using intermediate potentials (~ 0.3 V); and excellent for polymerisation potentials >0.4 V. There was also a trend in the latter range for further improvement with increasing polymerisation potential, which reached an optimum value when the PoPD electro-deposition was carried out at 0.7 V *vs.* SCE. However, little is known of the effects of the electropolymerisation potential on the mass of deposited PoPD or its thickness. Here we compare PoPD formed in neutral quiescent monomer solution, using either cyclic voltammetry, or amperometry at different fixed applied potentials, in terms of the mass of the PoPD layer deposited, using an electrochemical quartz-crystal microbalance (EQCM), and examine the relationship between this mass and permselectivity parameters relevant to H_2O_2-detecting biosensors.[21]

2. Experimental

2.1 Chemicals and solutions

ortho-Phenylenediamine (oPD) was obtained from Sigma–Aldrich Chemical Company, and used as supplied. Electropolymerisation of oPD was carried out in a phosphate buffered saline solution (PBS), pH 7.4, prepared by adding NaCl (Sigma, 150 mM), NaH_2PO_4 (Fluka, 40 mM) and NaOH (Fluka, 40 mM) to distilled water, bubbled with N_2 for 15 min and stored at 4 °C. A 100 mM monomer solution of oPD was prepared in 25 mL of PBS. This is close to the maximum concentration suitable for EQCM experiments, and avoids the precipitation of electropolymerisation by-products onto the upward-facing electrode which could give an overestimate of mass deposition.[76] Previous studies have shown that there is little difference between the interference rejection properties of PoPD formed at widely different concentrations,[77] and effective permselective PoPD layers are often generated from monomer solutions with concentrations as low as 5 mM[46,53,69,78,79] and 3 mM.[54,80] More recently, a within-study analysis showed that there was no statistically significant difference between the apparent AA permeability of PoPD formed from 10 mM and 300 mM (close to saturation) oPD.[81]

2.2 Instrumentation and software

An EQCM model 440 (CH Instruments, Austin, Texas, USA) electrochemical quartz-crystal microbalance was used. The cell and operational details have been described elsewhere,[49,56] although the performance of EQCM gold and platinum working electrodes (area 0.20 cm^2) was also compared here. Both constant potential amperometry (CPA) and a digital approximation (1 mV steps) of cyclic voltammetry (CV) were used in EQCM experiments, recording data using CH Instruments v2.06 software. For CV experiments, the applied potential range was 0–0.8 V *vs.* SCE at 20 mV s^{-1} for 10 scans, while recording simultaneously CV currents and the change in crystal oscillation frequency (see Fig. 1). For EQCM experiments employing CPA, fixed potential values (0.05, 0.15, 0.2, 0.25, 0.3, 0.4, 0.5, 0.6, 0.7 and 0.8 V *vs.* SCE) were applied for 15 min during which the current decay, associated with the self-sealing deposition of the insulating PoPD, and the change in oscillation frequency were recorded simultaneously. Statistical analyses and plots were performed using GraphPad Prism version 5.01 for Windows (GraphPad Software, San Diego, CA).

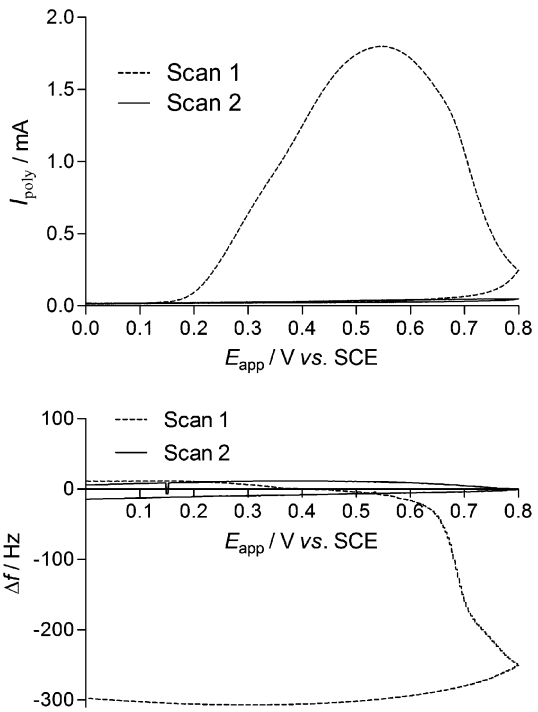

Fig. 1 (Top) CV of 100 mM oPD in the range 0–0.8 V *vs.* SCE at 20 mV s^{-1} for a quartz-crystal gold electrode, showing a collapse in current during the first scan. (Bottom) The concurrent change in oscillation frequency caused by PoPD electro-deposition. It is interesting to note that Δf did not become significant until ~ 0.6 V and then rapidly decreased until 0.8 V was reached. The Δf value then plateaued on the reverse scan, indicating near completion of the coating. Scan 2 and subsequent cycles did not show further change in frequency, again indicating that little or no further polymer deposition occurred.

2.3 Data analysis

The change in quartz-crystal oscillation frequency, Δf, reflects changes in mass and viscoelastic properties of the crystal/electrode/polymer surface; for the deposition of compact, insulating polymer films, however, Δf has been interpreted in terms of changes in mass alone.[82,83] This approximation is not valid for thick, conducting polymer films where phenomena such as viscoelastic effects, and exchange of counterions and solvent molecules, complicate the analysis.[84–86] For PoPD, under the conditions used here, both the voltammetric and QCM behavior shown in Fig. 1 are indicative of the formation of a compact and insulating polymeric film, blocking access of monomer to the surface. The formation of such an ultrathin layer meets the criteria of a rigid film (<10 nm; see Table 1) and permits the use of the Sauerbrey equation (eqn (4)),[87] *i.e.*, the observed frequency changes primarily reflect mass changes at the surface.[82–84] This was the approach adopted here, using eqn (4) to estimate the total added mass, Δm, on the electrode by measuring the final steady-state value of Δf, and then plotting Δm against the corresponding applied potential (see Fig. 2).

$$\Delta f = \frac{-2f_0^2}{A\sqrt{\mu\rho}}\Delta m \qquad (4)$$

Here f_0 is the fundamental resonant frequency of the crystal, A the area of the gold or platinum disk electrode coated onto the crystal, ρ the density of the crystal, and μ is the shear modulus of quartz. In the system used here these values were: f_0, 8.0 MHz; A, 0.20 cm^2; μ, 2.947 × 10^{11} g cm^{-1} s^{-2}; and ρ, 2.648 g cm^{-3}, giving a frequency change of 1 Hz for a mass change of 1.4 ng.

Assuming close packing of oligomer chains on the electrode surface allows the lower limit of polymer thickness to be estimated by calculation.[49] At least two factors might cause the actual thickness to be greater than that calculated here. Firstly, the polymer stands are unlikely to be all close packed; and secondly, the entrapment of solvent water molecules would lower the overall density of the film. However, this latter effect is likely to be less significant than for electrodeposited hydrophobic polymers in non-aqueous solvents.[84] Thus, although the values calculated for PoPD electrosynthesised at high anodic potentials (~4 nm; see Table 1) are in line with data published by others,[53] they are only estimates, and the primary focus is the total mass of the layer deposited during electrosynthesis. Two models were used here based on oligomers aligned either perpendicular or parallel to the electrode surface.[56] Using Δm values (eqn (4)), the thickness calculated for both models was similar, as expected from the assumption of close packing in the two cases. In reality, PoPD oligomers are likely to deposit over a range of angles on the surface but, because both 90° and 180° extremes yielded similar results,[56] the alignment distribution has little effect on the thickness of the layer. The mean thickness for the two models is therefore given in Table 1.

The efficiency of converting EQCM charge passed during electropolymerisation to mass deposited on the electrode was estimated by comparing the EQCM charge to the corresponding Δm values, as described recently.[56] The amount of charge passed during the polymerisation was calculated as the area under the current–time profile. The main assumption in calculating the charge efficiency was the number of electrons lost per monomer unit in forming the polymer chain. As discussed recently, the exact nature of polymerisation pathways and resulting bonding in the various PoPD strands is not known with certainty.[56,75] However, a z-value of 2 is not unreasonable for this estimate. The number of moles of monomer oxidised, and hence their mass, was computed from the charge passed. The efficiency of polymerisation process was estimated as the ratio of EQCM mass on the surface to this charge-calculated mass; see Table 1.

From current response *versus* concentration calibration plots for hydrogen peroxide (HP) and AA performed before and after deposition of PoPD onto Pt electrodes described recently,[75] a number of parameters were calculated to quantify the permeability and permselectivity of the polymer formed at different fixed applied potentials. The apparent analyte permeabilities to HP and AA were calculated, using eqn (5) and (6), respectively:[66,88]

$$P(\mathrm{HP})\% = \frac{\text{slope(HP) at Pt/PPD}}{\text{slope(HP) at bare Pt}} \times 100\% \qquad (5)$$

The slopes for the responses of HP on bare metal and on the PoPD-modified electrodes were obtained from the linear regression analysis of their respective calibration plots of the steady state HP current *versus* HP concentration. In contrast, AA calibrations for PoPD-modified electrodes are typically non-linear,[76,89] exhibiting a plateau over almost the entire

Table 1 Summary of EQCM data for ten applied electropolymerization potentials, with n = number of gold-coated electrodes. Mean ± SEM values were obtained for the change in oscillation frequency (Δf) from which the change in mass (Δm, eqn (4)), and the estimated minimum thickness calculated for close-packed arrangements of molecules on the electrode surface, were derived; see Section 2.3, which also outlines the calculation of charge efficiency

E_{app}/V *vs.* SCE	$-\Delta f$/Hz	Δm/ng	Thickness/nm	Charge efficiency (%)
0.80 (n = 2)	259 ± 1	357 ± 1	3.8 ± 0.1	2.8 ± 0.2
0.70 (n = 4)	252 ± 19	348 ± 26	3.7 ± 0.3	2.6 ± 0.3
0.60 (n = 2)	289 ± 6	399 ± 9	4.2 ± 0.1	2.9 ± 0.2
0.50 (n = 2)	243 ± 38	336 ± 52	3.5 ± 0.6	2.4 ± 0.4
0.40 (n = 6)	123 ± 13	169 ± 18	1.8 ± 0.2	0.8 ± 0.1
0.30 (n = 2)	79 ± 1	109 ± 2	1.2 ± 0.1	0.7 ± 0.1
0.25 (n = 2)	92 ± 27	127 ± 37	1.3 ± 0.4	0.7 ± 0.2
0.20 (n = 5)	54 ± 16	74 ± 23	0.8 ± 0.2	0.6 ± 0.2
0.15 (n = 3)	27 ± 4	37 ± 6	0.4 ± 0.1	0.3 ± 0.1
0.05 (n = 7)	2 ± 6	2 ± 6	N/A	N/A

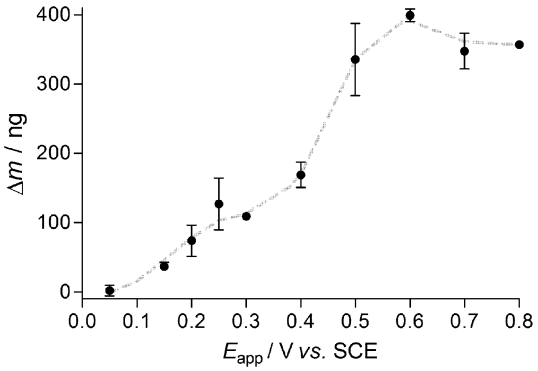

Fig. 2 Effect of applied electropolymerization potential on the total mass of PoPD deposited on EQCM electrodes. The main two trends highlighted are a steady increase in mass deposited in the potential range 0.1–0.5 V *vs.* SCE, followed by a plateau in PoPD total mass between 0.5 and 0.8 V. See Table 1 for *n*-values.

range of AA concentrations relevant to neurochemical applications (see Fig. 3). Hence the current at 1 mM AA (I_{AA}(1 mM)) was used as a measure of the relevant AA response. Values of $P(H_2O_2)$% and P(AA)%, calculated for individual electrodes and then averaged, reflect intrinsic properties of the PoPD which are normalised with respect to actual electrochemical surface area, rather than geometrically calculated area, and are ideally 100% and 0%, respectively, for biosensor applications.

$$P(\mathrm{AA})\% = \frac{I_{AA}(1\ \mathrm{mM})\ \mathrm{at\ Pt/PPD}}{I_{AA}(1\ \mathrm{mM})\ \mathrm{at\ bare\ Pt}} \times 100\% \qquad (6)$$

Polymer selectivity has been usefully defined as the percentage interference by AA in HP detection (eqn (7)),[76,89] with an optimum value of 0%. The use of equimolar concentrations of HP and AA in eqn (7), allows S% to be interpreted as the permselectivity of two analytes with an equal number of electrons transferred per molecule, as is the case here (z = 2). Although originally used to define the preferential permeation

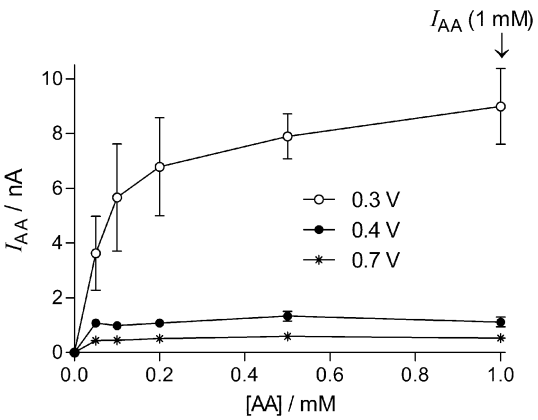

Fig. 3 Sample AA calibrations at 0.7 V *vs.* SCE for Pt/PoPD electropolymerised at three different applied potentials (*vs.* SCE): 0.3 V (n = 8), 0.4 V (n = 4) and 0.7 V (n = 19). Polymer formed at 0.3 V was much poorer at blocking AA than PoPD formed at 0.4 V and 0.7 V. Polymer electro-deposited at 0.7 V was significantly better at blocking AA than that formed at 0.4 V ($p < 0.001$), with a 2-fold lower I_{AA}(1 mM) value.

of ionic species through ion-exchange membranes (a phenomenon we might now call "ionic permselectivity"),[90,91] the generic term "permselectivity" has recently been applied more generally to quantify the ratio of permeabilities of both charged and uncharged species through any membrane structure.[46,57,66,92]

$$S\% = \frac{I_{AA}(1\ \mathrm{mM})\ \mathrm{at\ Pt/PPD}}{I_{HP}(1\ \mathrm{mM})\ \mathrm{at\ Pt/PPD}} \times 100\% \qquad (7)$$

Parameters are presented as mean ± standard error (SEM), with n = number of electrodes. The statistical significance of differences between values was calculated using the Student's two-tailed unpaired t-tests provided by GraphPad Prism (GraphPad Software, San Diego, CA).

3. Results and discussion

The ultra-thin nature of PPDs electrosynthesised at neutral pH has been widely reported,[49,50,53,79] and is consistent with their low conductivity and the consequent self-sealing nature of the process. Determination of the mass of the passivating, non-ionic form[93] of PoPD electro-deposited at different applied potentials was undertaken here to give further insight into the potential dependence of its permselective properties described recently.[75]

3.1 Comparison of gold- and platinum-coated quartz crystals

Previous within-study comparisons of PoPD deposited on gold, platinum, palladium and glassy-carbon electrodes indicated that there was little difference in the polymer permeability properties investigated.[94] However, because an aim in the present work was to compare data for PoPD deposited on EQCM gold electrodes with those for implantable Pt wire electrodes, a further comparison of the behaviour of these two substrates was undertaken here, *viz.* the mass of PoPD deposited on Au and Pt electrodes under the same electropolymerisation conditions. It would have been more straightforward to use Pt-coated quartz crystals throughout but the significantly higher cost of these predicated that, if no specific benefit could be demonstrated, then the cheaper Au-coated electrodes should be used.

Values of the initial (maximum) current and the final steady-state frequency change (Δf, eqn (4)) for oPD electropolymerisation, using CPA at 0.7 V *vs.* SCE, were used to compare the two metals. There was no statistically significant difference for either initial electropolymerisation current (Pt: 6.5 ± 0.5 mA, n = 5; and Au: 7.0 ± 0.2 mA, n = 4; $p > 0.5$) or final Δf values (Pt: 313 ± 74 Hz, n = 5; and Au: 252 ± 19 Hz, n = 4; $p > 0.45$). These results are consistent with the notion that the two noble metals act as inert conductors in the electropolymerisation of oPD and, in view of the potential window of these two electrode materials,[94] and the above-cited comparison of polymer permeability properties for PoPD deposited on gold and platinum, the use of gold-coated quartz crystals was deemed adequate for the remainder of this study.

3.2 Cyclic voltammetry, and EQCM

Fig. 1 shows an example of electro-deposition of PoPD onto a gold-coated EQCM electrode, driven by CV. Consistent with the conclusions in Section 3.1, the overall shape of the scan-1

current was similar to that observed for similar (high) concentrations of oPD on Pt wire electrodes,[75] displaying a shoulder at ~0.3 V followed by a sharp fall after 0.6 V. In line with this collapse in the scan-1 current, scan-2 (see Fig. 1) and subsequent scans were only marginally greater than the background current, a behaviour observed previously for this,[56] and other,[95,96] non-conducting electro-deposited coatings. The concurrently monitored change in oscillation frequency (Fig. 1, bottom) showed that the negative frequency change (mass increase) did not occur until ~0.6 V and accelerated until 0.8 V was reached. The Δf value then plateaued on the reverse scan, indicating no further polymer deposition. Scan 2 (Fig. 1) and subsequent scans did not show further change in frequency, again indicating little or no further mass deposition.

Although CV was useful in obtaining an overview of this process, the potential dependence of such a complex process is better investigated by studying the behaviour of the system at different fixed applied potentials (section 3.3). Nevertheless, even a superficial comparison of the CV current and mass deposited suggests that the majority of the current passed (especially up to 0.6 V in the forward sweep) did not produce species that were electro-deposited on the electrode surface. This is consistent with a charge efficiency analysis below, and highlights the limitation of using polymerisation charge alone to estimate the thickness of the electro-deposited layer.

3.3 Constant potential amperometry, and EQCM

Based on the shape of the CV shown in Fig. 1, ten different potential values were chosen to study the effect of fixed applied potential of the mass of PoPD deposited. Table 1 lists the values for the maximum change in oscillation frequency (Δf), the associated change in mass (Δm, eqn (4)) and estimated deposition thickness (d) for electropolymerisation at these potentials; see Section 2.3. From Table 1 the estimated *minimum* thickness for the polymer formed at 0.7 V *vs.* SCE was 3.7 ± 0.3 nm (n = 4), which agrees with previous values reported in the literature of <10 nm,[53,76,97–99] and was not significantly different from values determined in the range 0.5–0.8 V. It is also worth noting that the change in frequency obtained for the electropolymerisation of oPD at fixed potential values between 0.5 and 0.8 V was similar to the maximum frequency change observed for the CV method (~300 Hz; see Fig. 1).

Fig. 2 shows the effect of applied electropolymerisation potential on the total mass of PoPD deposited. The overall shape resembles that of the CV scan-1 forward sweep current up to ~0.6 V (Fig. 1), with a shoulder before more significant deposition at higher applied potentials. One might expect the plot in Fig. 2 to correspond more closely to the Δf plot in Fig. 1. However, this highlights the complexity of interpreting the evolution of mass when the applied potential is changing continuously. For example, Fig. 2 indicates that mass is deposited for fixed applied electropolymerisation potentials as low as 0.15 V *vs.* SCE, whereas significant mass was not observed until ~0.6 V when the scan rate was 20 mV s^{-1}. The two main statistical trends highlighted by Fig. 2 are a steady increase in mass deposited in the potential range 0.1–0.5 V *vs.* SCE, followed by a plateau in PoPD total mass between 0.5 and 0.8 V.

The efficiency of converting charge passed to mass deposited on the electrode was estimated by comparing the electropolymerisation charge to the EQCM mass on the surface (section 2.3).[56,83] Although the accuracy of the absolute value of this "charge efficiency" is open to debate (*e.g.*, the adoption of an assumed z-value for the process), the parameter has proved useful in comparing trends in related systems. For example, in a previous study which compared the electropolymerisation behaviour of the three isomers of phenylenediamine,[56] the charge conversion efficiency was similar for oPD and pPD, but significantly greater for mPD, which was consistent with the formation of solution precipitates for oPD and pPD, but not the *meta* isomer, during the electropolymerisation process. For PoPD electro-deposited here at different fixed applied potentials, even the maximum charge efficiency (observed between 0.8 and 0.5 V *vs.* SCE) was very low (~3%; see Table 1). The values between 0.4 and 0.2 V were also similar to each other, but significantly lower (~0.7%) than for the higher applied potentials. Taken together, these very low charge efficiency values highlight the limitation of using polymerisation charge alone to estimate the thickness of the electro-deposited layer. For example, even for the highest efficiency observed in the present study, the use of electropolymerisation charge would yield a ~30-fold overestimate of deposited mass, and hence derived thickness.

3.4 Influence of PoPD layer mass on its permselective properties

An important goal in recent biosensor research is the fabrication of amperometric microsensors suitable for tissue implantation *in vivo*,[22,100–104] especially for brain monitoring.[21,105–108] These implantable devices must be able to reject electrochemical interference by reducing agents present in the tissue, and a common strategy is the incorporation of a permselective membrane such as PoPD in the biosensor design.[109–115] This polymer is unusual[50] in that it displays very high permeability to the biosensor signal transduction molecule (H_2O_2, see reactions (2) and (3)) while being remarkably effective at blocking a variety of interference molecules,[45–47,49,56,116] especially AA which is present in many biological fluids at significantly higher concentrations than other interference species. For example, P(AA)% values (eqn (6)) of less than 0.1% have been reported recently for PoPD-modified Pt wire and fiber electrodes.[66,116]

The transport of analytes from solution through an insulating polymer coating on an electrode to the underlying metal substrate is a complex process.[117,118] Parameters involved in membrane transport include the permeant's partition and diffusion coefficients in the polymer, as well as polymer thickness.[93,119] Because the thickness of the non-conducting form of PoPD generated under the electrodeposition conditions used in the present work is not known accurately, the "true permeability" of an analyte cannot be determined in a straightforward manner.[119] Instead, we have defined the "apparent permeability" of an analyte (eqn (5) and (6)) as the ratio of the analyte currents recorded with the same

electrode before and after deposition of the polymer. The apparent permeability is a relative, normalised measure of the analyte flux to the metal surface when the polymer coating is present, and this parameter has proved useful in comparing the properties of permselective polymers for biosensor applications.[21,56] Permselectivity data for PoPD electrosynthesised at the different applied potentials were compared with the mass profile determined here (Fig. 2) to see whether further insight into the factors affecting the permeability of these PoPD coatings could be obtained.

Fig. 3 shows examples of AA calibrations for Pt/PoPD electrodes formed at different electropolymerisation potentials. Even for electro-deposition potentials as low as 0.3 V *vs.* SCE, the PoPD formed showed good AA blocking ability, manifested by a value of I_{AA} (1 mM) of 9.9 ± 1.4 nA (n = 8), which compared with the bare metal value of ~600 nA. Also evident was the distinctive nonlinear response to AA displayed by PoPD formed at the more common higher applied potentials.[56,75] Specifically, there was a plateau region over most of the AA concentration range, which was chosen for its neurochemical relevance.[21] The PoPD formed at 0.4 V exhibited ~10-fold greater blocking of AA compared with that formed at 0.3 V (Fig. 3), although there was no significant difference in the mass deposited for applied potentials in the range 0.25 to 0.4 V (see Table 1 and Fig. 2). Moreover, the polymer deposited at 0.7 V showed a significantly lower permeability to AA compared with that formed at 0.4 V ($p < 0.001$), with a 2-fold lower I_{AA}(1 mM) value; see Fig. 3. The potential dependence of P(AA)% for PoPD has been discussed at some length recently.[75] The main novelty in the present work was to examine how the mass of deposited PoPD related to its permeability parameters. This was achieved by matching (on the basis of the applied potential used for the electropolymerisation) EQCM mass density with permeability parameters determined for Pt/PoPD wire electrodes. This was necessary because the 2-sided EQCM electrodes were not amenable to reliable analyte calibration. Furthermore, the similarity between the behaviour of Au and Pt electrodes in Section 3.1, coupled with the small PoPD "edge density" of the EQCM and wire geometries,[66] provides some justification for this comparison.

Overlaying the full AA calibration plots for all ten mass densities obtained would be unwieldy. Instead, the I_{AA}(1 mM) values (see Fig. 3) for each set were used to calculate P(AA)%, using eqn (6), which were then plotted against PoPD mass density (Fig. 4, top). For mass densities less than ~0.4 μg cm^{-2}, there was virtually no blocking of AA access to the electrode with P(AA)% values >80%. Surprisingly, PoPD masses just slightly greater than this value (~0.6 μg cm^{-2}) displayed 40-times lower AA permeability (~2% of the response for the bare metal), and there was a further quantal decrease in P(AA)% to ~0.4% at PoPD masses of ~0.8 μg cm^{-2}. For greater mass values, there was a minor decrease in P(AA)% which reached a minimum (optimum for biosensor applications) of 0.11 ± 0.02% at ~1.8 μg cm^{-2} (Fig. 4, top inset).

As AA permeability decreased with increasing mass of electro-deposited PoPD, the H_2O_2 permeability surprisingly increased (Fig. 4, bottom), and P(HP)% reached bare metal values for masses of ~2 μg cm^{-2}, in line with published data for PoPD generated at the high electropolymerisation potentials needed to deposit this level of mass.[45,49,56,60,66,116,120] The physicochemical basis of the efficient transport of H_2O_2 through PoPD coatings on electrode surfaces (P(HP)% ≈ 100%) has not been established, although this property is shared by PmPD and PpPD,[46,56] but not by other aromatic diamines.[50] In contrast, for example, the equivalent P(HP)% value for polyphenol has been estimated at <10%.[121] The finding here that P(HP)% increased with the mass of the PoPD layer adds further to the enigma, but may help later in understanding the behaviour of H_2O_2 at PoPD-modified electrodes.

Irrespective of the mechanisms underlying the transport of H_2O_2 through PoPD and its ability to block AA access to the underlying metal substrate, both these phenomena are key to the success of PoPD as a permselective layer in biosensor applications. Combining the responses for AA and H_2O_2 in the form of the selectivity parameter, S% (eqn (7)), is superior to the direct ratio of the P(AA)% and P(HP)%,[56] because S% is determined solely by the properties of the polymer-modified electrode, and does not have contributions from the unmodified bare metal, whose calibration parameters can show a greater coefficient of variation.[45] Because of the huge range of P(AA)% values observed (90–0.1%) over the range of PoPD mass deposited (Fig. 4, top) compared with that for P(HP)% (100–60%, Fig. 4, bottom), the dependence of S% on polymer mass was dominated by AA permeability factors (Fig. 5). For mass densities less than ~0.4 μg cm^{-2}, the selectivity was poor with an S% value of ~70%. This is similar to the bare-metal S% value, which is not 100% because of the difference in the diffusion coefficients for AA and H_2O_2.[45] PoPD masses of ~0.6 μg cm^{-2} displayed 40-times greater selectivity (~1.7%), and there was a further abrupt decrease in S% to ~0.2% at ~0.8 μg cm^{-2} PoPD. A minimum (optimum for biosensor applications) was reached of 0.09 ± 0.01% at ~1.8 μg cm^{-2} (Fig. 5, *inset*).

Further insights into the structure and properties of electro-deposited PoPD layers might be obtained from a range of techniques, such as scanning electrochemical and atomic force microscopies.[122–125] For example, interesting aspects of the surface structure of PPDs[56,120,126] and other electro-deposited polymers[127–129] have been revealed in the past by scanning electron microscopy. However, the topography of two forms of PoPD generated in a recent study (using either CV or a fixed applied potential of 700 mV *vs.* SCE: Pt/PoPD$_{CV}$ and Pt/PoPD$_{700}$), which displayed very different AA calibration responses, was only marginally different.[75] It is worth noting that the mass of the same two forms of PoPD determined here was also similar (Section 3.3). These similarities in mass and topography for Pt/PoPD$_{CV}$ and Pt/PoPD$_{700}$ highlight the sensitivity of apparent permeabilities, especially P(AA)%, in revealing differences between PoPD layers electro-deposited under different conditions. In addition to the level of sensitivity afforded by these parameters, it is the same permeability properties that are exploited in the design of permselective biosensors and are therefore most apt for their functional characterisation.

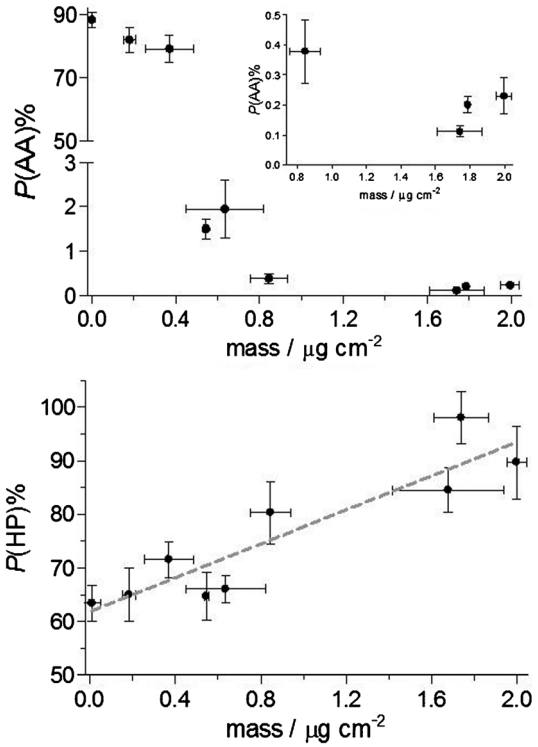

Fig. 4 Plots of apparent permeabilities, *P*(HP)% from eqn (5) (bottom), and *P*(AA)% from eqn (6) (top), against mass density of the PoPD layer. Linear regression analysis of the *P*(HP)% plot showed that the slope was statistically significant ($R^2 = 0.83$ with $p < 0.001$).

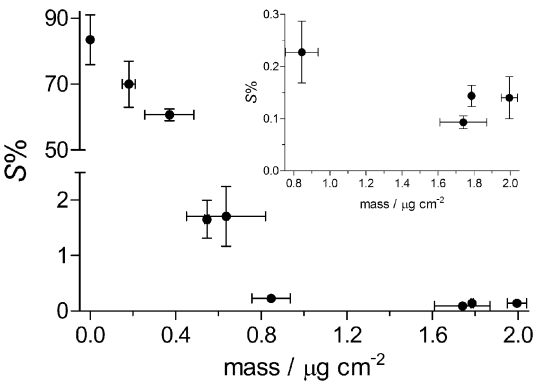

Fig. 5 Plots of *S*% values (eqn (7)) against mass density of the PoPD layer. *Inset*: Close-up of main graph showing that the lowest (best) *S*% value ($0.09 \pm 0.01\%$ at ~ 1.8 μg cm^{-2}) was significantly different from the value at ~ 0.8 μg cm^{-2} ($0.23 \pm 0.06\%$, $p < 0.003$).

4. Conclusions

Comparison of PoPD deposited on Pt and Au electrodes at a fixed applied potential in terms of electropolymerisation currents, layer mass, and reported permeability data indicated that the behaviour of the two noble metal substrates was similar in this context. This allowed a wider comparison of the potential dependence of polymer mass recorded here for Au/PoPD electrodes with a large literature pool of Pt/PoPD permselectivity parameters. There was a steady increase in PoPD mass deposited for fixed applied potentials from 0.05 to 0.6 V *vs.* SCE, followed by a plateau up to 0.8 V (Fig. 2). The apparent permeability for AA, the archetypal biosensor interference species, decreased with increasing PoPD mass, but the relationship was more stepwise than smooth, major decreases observed at ~ 0.4 and 0.6 μg cm^{-2} (Fig. 4, top). In contrast, *P*(HP)% values appeared to change linearly with mass of PoPD deposited over the applied potential range studied, but in this case the change was contrary to expectation, *P*(HP)% increasing as additional mass was deposited (Fig. 4, bottom). This is further evidence that, for cases where *P*-values do not vary far from 100% (in contrast to *P*(AA)% which can be as low as 0.1%), *P*(HP)% is not as much a permeability parameter as an index of the chemistry of this labile molecule at the electrode surface.[75]

Overall the results indicate that the ability of the passivating form of PoPD to block interference species in biosensor applications is not related in a simple way to the mass of material deposited on the surface. Instead, effects of the applied electropolymerisation potential in driving the electro-oxidation of oPD dimers and oligomers formed during the electro-deposition process are likely to have a more direct impact on the selectivity characteristics of the PoPD layer.[69,75] The results also highlight the sensitivity of apparent permeabilities, especially *P*(AA)%, in revealing differences between PoPD layers electro-deposited under different conditions.

Acknowledgements

This work was funded in part by the Irish Research Council for Science, Engineering and Technology (IRCSET), and by University College Dublin.

References

1 L. C. Clark, Jr. and C. Lyons, *Ann. N. Y. Acad. Sci.*, 1962, **102**, 29.
2 R. A. Kamin and G. S. Wilson, *Anal. Chem.*, 1980, **52**, 1198.
3 W. J. Albery and P. N. Bartlett, *J. Electroanal. Chem.*, 1985, **194**, 211.
4 E. R. Hirst, Y. J. Yuan, W. L. Xu and J. E. Bronlund, *Biosens. Bioelectron.*, 2008, **23**, 1759.
5 A. K. Wanekaya, W. Chen and A. Mulchandani, *J. Environ. Monit.*, 2008, **10**, 703.
6 O. A. Sadik, A. O. Aluoch and A. L. Zhou, *Biosens. Bioelectron.*, 2009, **24**, 2749.
7 N. Sozer and J. L. Kokini, *Trends Biotechnol.*, 2009, **27**, 82.
8 H. Saito, T. Nakazato, N. Ishii, H. Kudo, K. Otsuka, H. Endo and K. Mitsubayashi, *Eur. Food Res. Technol.*, 2007, **227**, 473.
9 P. V. Bernhardt, *Aust. J. Chem.*, 2006, **59**, 233.
10 Z. Xu, X. Chen and S. J. Dong, *TrAC, Trends Anal. Chem.*, 2006, **25**, 899.
11 L. Murphy, *Curr. Opin. Chem. Biol.*, 2006, **10**, 177.
12 L. Stoica, R. Ludwig, D. Haltrich and L. Gorton, *Anal. Chem.*, 2006, **78**, 393.
13 X. J. Tang, B. Xie, P. O. Larsson, B. Danielsson, M. Khayyami and G. Johansson, *Anal. Chim. Acta*, 1998, **374**, 185.
14 R. J. O. Cosford and W. G. Kuhr, *Anal. Chem.*, 1996, **68**, 2164.
15 S. Kuwabata, *Chem. Lett.*, 2008, **37**, 230.
16 S. Chakraborty and C. R. Raj, *Electrochem. Commun.*, 2007, **9**, 1323.
17 Y. Q. Lin, K. Liu, P. Yu, L. Xiang, X. C. Li and L. Q. Mao, *Anal. Chem.*, 2007, **79**, 9577.
18 H. Wei and E. Wang, *Anal. Chem.*, 2008, **80**, 2250.
19 R. A. Doong and H. M. Shih, *Biosens. Bioelectron.*, 2006, **22**, 185.
20 F. Davis and S. P. J. Higson, *Biosens. Bioelectron.*, 2005, **21**, 1.
21 R. D. O'Neill, J. P. Lowry, G. Rocchitta, C. P. McMahon and P. A. Serra, *TrAC, Trends Anal. Chem.*, 2008, **27**, 78.

22 P. Pernot, J. P. Mothet, O. Schuvailo, A. Soldatkin, L. Pollegioni, M. Pilone, M. T. Adeline, R. Cespuglio and S. Marinesco, *Anal. Chem.*, 2008, **80**, 1589.
23 J. Wang, *Chem. Rev.*, 2008, **108**, 814.
24 D. Foxx and E. E. Kalu, *Electrochem. Commun.*, 2007, **9**, 584.
25 R. Maalouf, H. Chebib, Y. Saikali, O. Vittori, M. Sigaud, F. Garrelie, C. Donnet and N. Jaffrezic-Renault, *Talanta*, 2007, **72**, 310.
26 A. S. Khan and A. C. Michael, *TrAC, Trends Anal. Chem.*, 2003, **22**, 503.
27 G. S. Wilson and R. Gifford, *Biosens. Bioelectron.*, 2005, **20**, 2388.
28 G. S. Wilson and Y. B. Hu, *Chem. Rev.*, 2000, **100**, 2693.
29 R. D. O'Neill, J. P. Lowry and M. Mas, *Crit. Rev. Neurobiol.*, 1998, **12**, 69.
30 P. Pantano and W. G. Kuhr, *Electroanalysis*, 1995, **7**, 405.
31 Y. Li and H. E. Schellhorn, *J. Nutrition*, 2007, **137**, 2171.
32 C. H. Lee, S. C. Wang, C. J. Yuan, M. F. Wen and K. S. Chang, *Biosens. Bioelectron.*, 2007, **22**, 877.
33 M. A. Rahman, N. H. Kwon, M. S. Won, E. S. Choe and Y. S. Shim, *Anal. Chem.*, 2005, **77**, 4854.
34 J. Kulys and A. Drungiliene, *Electroanalysis*, 1991, **3**, 209.
35 S. P. Perone and W. J. Kretlow, *Anal. Chem.*, 1966, **38**, 1760.
36 J. Wang, J. Liu, L. Chen and F. Lu, *Anal. Chem.*, 1994, **66**, 3600.
37 J. Wang, F. Lu, L. Angnes, J. Liu, H. Sakslund, Q. Chen, M. Pedrero, L. Chen and O. Hammerich, *Anal. Chim. Acta*, 1995, **305**, 3.
38 M. A. Rahman, M. S. Won and Y. B. Shim, *Electroanalysis*, 2007, **19**, 631.
39 T. Tatsuma and N. Oyama, *Anal. Chem.*, 1996, **68**, 1612.
40 A. A. Karyakin, *Electroanalysis*, 2001, **13**, 813.
41 P. Salazar, M. Martin, R. Roche, R. D. O'Neill and J. L. Gonzalez-Mora, *Electrochim. Acta*, 2010, **55**, 6476.
42 P. Salazar, M. Martin, R. Roche, J. L. Gonzalez-Mora and R. D. O'Neill, *Biosens. Bioelectron.*, 2010, **26**, 748.
43 S. Cosnier, *Anal. Lett.*, 2007, **40**, 1260.
44 N. Hamdi, J. J. Wang, E. Walker, N. T. Maidment and H. G. Monbouquette, *J. Electroanal. Chem.*, 2006, **591**, 33.
45 S. M. Kirwan, G. Rocchitta, C. P. McMahon, J. D. Craig, S. J. Killoran, K. B. O'Brien, P. A. Serra, J. P. Lowry and R. D. O'Neill, *Sensors*, 2007, **7**, 420.
46 Y. Q. Dai, D. M. Zhou and K. K. Shiu, *Electrochim. Acta*, 2006, **52**, 297.
47 O. M. Schuvailo, O. O. Soldatkin, A. Lefebvre, R. Cespuglio and A. P. Soldatkin, *Anal. Chim. Acta*, 2006, **573–574**, 110.
48 C. P. McMahon, S. J. Killoran, S. M. Kirwan and R. D. O'Neill, *Chem. Commun.*, 2004, 2128.
49 J. D. Craig and R. D. O'Neill, *Analyst*, 2003, **128**, 905.
50 L. J. Murphy, *Anal. Chem.*, 1998, **70**, 2928.
51 I. Losito and C. G. Zambonin, *J. Electroanal. Chem.*, 1996, **410**, 181.
52 J. M. Cooper, P. L. Foreman, A. Glidle, T. W. Ling and D. J. Pritchard, *J. Electroanal. Chem.*, 1995, **388**, 143.
53 C. Malitesta, F. Palmisano, L. Torsi and P. G. Zambonin, *Anal. Chem.*, 1990, **62**, 2735.
54 S. V. Sasso, R. J. Pierce, R. Walla and A. M. Yacynych, *Anal. Chem.*, 1990, **62**, 1111.
55 S. J. Killoran, D. K. Rai and R. D. O'Neill, *J. Neurochem.*, 2007, **102**, 196.
56 S. J. Killoran and R. D. O'Neill, *Electrochim. Acta*, 2008, **53**, 7303.
57 M. H. Pournaghi-Azar and B. Habibi, *J. Electroanal. Chem.*, 2007, **601**, 53.
58 E. Dempsey, J. Wang and M. R. Smyth, *Talanta*, 1993, **40**, 445.
59 P. N. Bartlett and P. R. Birkin, *Anal. Chem.*, 1994, **66**, 1552.
60 J. P. Lowry, K. McAteer, S. S. El Atrash, A. Duff and R. D. O'Neill, *Anal. Chem.*, 1994, **66**, 1754.
61 K. McAteer and R. D. O'Neill, *Analyst*, 1996, **121**, 773.
62 P. N. Bartlett, J. H. Wang and W. James, *Analyst*, 1998, **123**, 387.
63 J. I. Reyes De Corcuera, R. P. Cavalieri and J. R. Powers, *J. Electroanal. Chem.*, 2005, **575**, 229.
64 C. P. McMahon, G. Rocchitta, S. M. Kirwan, S. J. Killoran, P. A. Serra, J. P. Lowry and R. D. O'Neill, *Biosens. Bioelectron.*, 2007, **22**, 1466.
65 G. Calia, G. Rocchitta, R. Migheli, G. M. Puggioni, Y. Spissu, G. Bazzu, V. Mazzarello, J. P. Lowry, R. D. O'Neill, M. S. Desole and P. A. Serra, *Sensors*, 2009, **9**, 2511.
66 S. A. Rothwell, M. E. Kinsella, Z. M. Zain, P. A. Serra, G. Rocchitta, J. P. Lowry and R. D. O'Neill, *Anal. Chem.*, 2009, **81**, 3911.
67 X. G. Li, M. R. Huang, W. Duan and Y. L. Yang, *Chem. Rev.*, 2002, **102**, 2925.
68 D. H. Jang, Y. S. Yoo and S. M. Oh, *Bull. Kor. Chem. Soc.*, 1995, **16**, 392.
69 I. Losito, F. Palmisano and P. G. Zambonin, *Anal. Chem.*, 2003, **75**, 4988.
70 M. A. del Valle, F. R. Diaz, M. E. Bodini, G. Alfonso, G. M. Soto and E. D. Borrego, *Polym. Int.*, 2005, **54**, 526.
71 L. L. Wu, J. Luo and Z. H. Lin, *J. Electroanal. Chem.*, 1997, **440**, 173.
72 I. Losito, E. De Giglio, N. Cioffi and C. Malitesta, *J. Mater. Chem.*, 2001, **11**, 1812.
73 T. Komura, Y. Funahasi, T. Yamaguti and K. Takahasi, *J. Electroanal. Chem.*, 1998, **446**, 113.
74 E. Ekinci, G. Erdogdu and A. E. Karagozler, *J. Appl. Polym. Sci.*, 2001, **79**, 327.
75 S. A. Rothwell, C. P. McMahon and R. D. O'Neill, *Electrochim. Acta*, 2010, **55**, 1051.
76 S. J. Killoran and R. D. O'Neill, *Electrochim. Acta*, 2008, **53**, 7303.
77 M. R. Ryan, J. P. Lowry and R. D. O'Neill, *Analyst*, 1997, **122**, 1419.
78 B. A. Patel, M. Arundell, K. H. Parker, M. S. Yeoman and D. O'Hare, *Anal. Chem.*, 2006, **78**, 7643.
79 S. Myler, S. Eaton and S. P. J. Higson, *Anal. Chim. Acta*, 1997, **357**, 55.
80 N. Hamdi, J. J. Wang and H. G. Monbouquette, *J. Electroanal. Chem.*, 2005, **581**, 258.
81 S. A. Rothwell, S. J. Killoran and R. D. O'Neill, *Sensors*, 2010, **10**, 6439.
82 D. A. Buttry and M. R. Deakin, *Anal. Chem.*, 1989, **61**, 1147A.
83 J. Wang, M. Jiang and F. Lu, *J. Electroanal. Chem.*, 1998, **444**, 127.
84 M. Skompska, A. Jackson and A. R. Hillman, *Phys. Chem. Chem. Phys.*, 2000, **2**, 4748.
85 M. A. Mohamoud and A. R. Hillman, *J. Solid State Electrochem.*, 2007, **11**, 1043.
86 A. R. Hillman, Q. Z. Dong, M. A. Mohamoud and I. Efimov, *Electrochim. Acta*, 2010, **55**, 8142.
87 G. Sauerbrey, *Z. Phys.*, 1959, **155**, 206.
88 R. D. O'Neill, J. P. Lowry, G. Rocchitta, C. P. McMahon and P. A. Serra, *TrAC, Trends Anal. Chem.*, 2008, **27**, 78.
89 S. A. Rothwell, M. E. Kinsella, Z. M. Zain, P. A. Serra, G. Rocchitta, J. P. Lowry and R. D. O'Neill, *Anal. Chem.*, 2009, **81**, 3911.
90 C. F. Shu and F. C. Anson, *J. Am. Chem. Soc.*, 1990, **112**, 9227.
91 J. Wang and T. Golden, *Anal. Chem.*, 1989, **61**, 1397.
92 F. Palmisano, C. Malitesta, D. Centonze and P. G. Zambonin, *Anal. Chem.*, 1995, **67**, 2207.
93 D. Centonze, C. Malitesta, F. Palmisano and P. G. Zambonin, *Electroanalysis*, 1994, **6**, 423.
94 R. D. O'Neill, S. C. Chang, J. P. Lowry and C. J. McNeil, *Biosens. Bioelectron.*, 2004, **19**, 1521.
95 A. Guerrieri, R. Ciriello and D. Centonze, *Biosens. Bioelectron.*, 2009, **24**, 1550.
96 A. E. Fischer, T. M. Mcevoy and J. W. Long, *Electrochim. Acta*, 2009, **54**, 2962.
97 Y. Ohnuki, H. Matsuda, T. Ohsaka and N. Oyama, *J. Electroanal. Chem.*, 1983, **158**, 55.
98 T. W. Sohn, P. W. Stoecker, W. Carp and A. M. Yacynych, *Electroanalysis*, 1991, **3**, 763.
99 J. M. Cooper and D. J. Pritchard, *J. Mater. Sci.-Mater. Electron.*, 1994, **5**, 111.
100 F. Ahmad, A. P. M. Yusof, M. Bainbridge and S. Ab Ghani, *Biosens. Bioelectron.*, 2008, **23**, 1862.
101 J. J. Burmeister, F. Pomerleau, P. Huettl, C. R. Gash, C. E. Wemer, J. P. Bruno and G. A. Gerhardt, *Biosens. Bioelectron.*, 2008, **23**, 1382.
102 J. F. Masson, C. Kranz, B. Mizaikoff and E. B. Gauda, *Anal. Chem.*, 2008, **80**, 3991.
103 K. M. Wassum, V. M. Tolosa, J. J. Wang, E. Walker, H. G. Monbouquette and N. T. Maidment, *Sensors*, 2008, **8**, 5023.

104 N. V. Kulagina and A. C. Michael, *Anal. Chem.*, 2003, **75**, 4875.
105 M. van der Zeyden, W. H. Denziel, K. Rea, T. I. Cremers and B. H. Westerink, *Pharmacol., Biochem. Behav.*, 2008, **90**, 135.
106 G. S. Wilson and M. A. Johnson, *Chem. Rev.*, 2008, **108**, 2462.
107 N. Dale, S. Hatz, F. M. Tian and E. Llaudet, *Trends Biotechnol.*, 2005, **23**, 420.
108 J. J. Burmeister and G. A. Gerhardt, *TrAC, Trends Anal. Chem.*, 2003, **22**, 498.
109 Y. C. Fu, C. Chen, Q. J. Xie, X. H. Xu, C. Zou, Q. M. Zhou, L. Tan, H. Tang, Y. Y. Zhang and S. Z. Yao, *Anal. Chem.*, 2008, **80**, 5829.
110 K. B. O'Brien, S. J. Killoran, R. D. O'Neill and J. P. Lowry, *Biosens. Bioelectron.*, 2007, **22**, 2994.
111 C. P. McMahon, G. Rocchitta, P. A. Serra, S. M. Kirwan, J. P. Lowry and R. D. O'Neill, *Anal. Chem.*, 2006, **78**, 2352.
112 J. I. Reyes-De-Corcuera, R. P. Cavalieri, J. R. Powers, J. M. Tang and D. H. Kang, *J. Agric. Food Chem.*, 2005, **53**, 8866.
113 Y. Q. Dai and K. K. Shiu, *Electroanalysis*, 2004, **16**, 1806.
114 T. Yao, T. Yano, Y. Nanjyo and H. Nishino, *Anal. Sci.*, 2003, **19**, 61.
115 P. N. Bartlett, P. R. Birkin, J. H. Wang, F. Palmisano and G. Debenedetto, *Anal. Chem.*, 1998, **70**, 3685.
116 S. A. Rothwell, S. J. Killoran, E. M. Neville, A. M. Crotty and R. D. O'Neill, *Electrochem. Commun.*, 2008, **10**, 1078.
117 T. Ikeda, R. Schmehl, P. Denisevich, K. Willman and R. W. Murray, *J. Am. Chem. Soc.*, 1982, **104**, 2683.
118 J. M. Saveant, *J. Electroanal. Chem.*, 1991, **302**, 91.
119 R. Pyati and R. W. Murray, *J. Phys. Chem.*, 1994, **98**, 11129.
120 J. P. Lowry and R. D. O'Neill, *Electroanalysis*, 1994, **6**, 369.
121 J. D. Craig and R. D. O'Neill, *Anal. Chim. Acta*, 2003, **495**, 33.
122 D. W. M. Arrigan and P. N. Bartlett, *Biosens. Bioelectron.*, 1998, **13**, 293.
123 Y. D. Wang, P. P. Joshi, K. L. Hobbs, M. B. Johnson and D. W. Schmidtke, *Langmuir*, 2006, **22**, 9776.
124 A. M. Tenreiro, C. Nabais, J. P. Correia, F. M. S. S. Fernandes, J. R. Romero and L. M. Abrantes, *J. Solid State Electrochem.*, 2007, **11**, 1059.
125 D. Grieshaber, R. MacKenzie, J. Voros and E. Reimhult, *Sensors*, 2008, **8**, 1400.
126 J. Wang, Q. Chen, C. L. Renschler and C. White, *Anal. Chem.*, 1994, **66**, 1988.
127 P. N. Bartlett, D. Pletcher and J. Zeng, *J. Electrochem. Soc.*, 1997, **144**, 3705.
128 U. Yogeswaran and S. M. Chen, *Sens. Actuators, B*, 2008, **130**, 739.
129 F. J. Shang, Y. L. Liu, S. Hrapovic, J. D. Glennon and J. H. T. Luong, *Analyst*, 2009, **134**, 519.